VERSITA

Acta Geophysica
vol. 56, no. 2, pp. 417-439
DOI: 10.2478/s11600-007-0046-y

SWAT.nz: New-Zealand-based "Sand Waves and Turbulence" experimental programme

Stephen E. COLEMAN[1], Vladimir I. NIKORA[2], Bruce W. MELVILLE[1], Derek G. GORING[3], Thomas M. (Dougal) CLUNIE[1], and Heide FRIEDRICH[1]

[1]Department of Civil and Environmental Engineering, The University of Auckland, Auckland, New Zealand
e-mails: s.coleman@auckland.ac.nz, b.melville@auckland.ac.nz, tclu001@ec.auckland.ac.nz, h.friedrich@auckland.ac.nz

[2]Department of Engineering, University of Aberdeen, Aberdeen, United Kingdom
e-mail: v.nikora@abdn.ac.uk

[3]Mulgor Consulting Ltd., Riccarton, Christchurch, New Zealand
e-mail: d.goring@mulgor.co.nz

A b s t r a c t

The SWAT.nz ("New-Zealand-based Sand Waves and Turbulence") research programme was carried out to advance understanding of subaqueous sand waves. The programme was based around detailed measurements at varying scales of bed morphologies and associated flow fields as sand waves formed from plane-bed conditions and grew to equilibrium.

This paper outlines the philosophy and details of the SWAT.nz programme, with the aim of providing insight into experiment and analysis design and methodologies for studies of highly-variable bed surfaces and flows. Example challenges addressed in the SWAT.nz programme include the measurement over large spatial domains of developing flow fields and three-dimensional bed morphology, including flow measurements below roughness (sand-wave) crests, and how to interpret the collected measurements. Insights into sand-wave dynamics that have arisen from the programme are presented to illustrate the values of the SWAT.nz programme and the developed methodologies. Results are presented in terms of mobile-bed processes, and flow-bed interaction and flow processes for fixed-bed roughness and erodible beds, respectively.

Key words: sediment, sand wave, ripple, dune, turbulence.

1. INTRODUCTION

When water flows over a particulate bed causing particles to move, regular patterns of waves develop in the bed. Waves in sediment beds beneath tranquil water flows are typically described as ripples or dunes (Fig. 1), ripples being small fine-sediment bed waves that do not influence the water surface, and dunes being bed waves that occupy a significant portion of the flow depth, causing the water surface to be disturbed (ASCE 1966). Flow over a planar sediment bed gives the origin of both of these bed waves as small sand wavelets, different mechanisms acting to grow ripples or dunes, respectively, for the flow (Coleman and Melville 1996). Both ripples and dunes grow at rates reducing with time (e.g., Nikora and Hicks 1997, Coleman *et al.* 2005b) to attain magnitudes in equilibrium with the applied flow. These magnitudes are typically described as a function of sediment properties for ripples (e.g., Raudkivi 1997), and flow properties (principally) for dunes (e.g., Yalin 1992). Ripples and dunes are common features of river beds, sea floors, geological strata, and many hydro-transport engineering systems. These wave trains are intriguing to the eye, and significant to the environment in controlling scour, hyporheic flows (e.g., Packman *et al.* 2004, Marion *et al.* 2002), and movement of the granular particles and any attached contaminants (including organic molecules, inorganics, and disease-carrying micro-organisms).

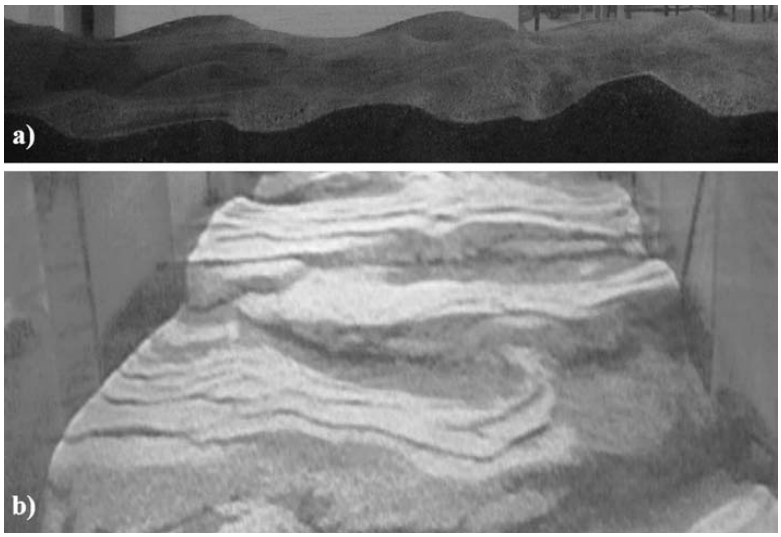

Fig. 1. Example SWAT.nz sand waves: (a) fine-sediment ripples in the narrow flume, (b) coarse-sediment dunes in the wide flume.

With nice insight building on earlier works, coupled with accelerations in the abilities of laboratory and field instrumentation, notable advances have been made over the past decades concerning understanding of fluid flow and sediment dynamics over bed waves (e.g., Lyn 1993, Nelson *et al.* 1993, Bennett and Best 1995, Coleman and Melville 1996, Kostaschuk and Villard 1996, Nikora *et al.* 1997, McLean *et al.*

1999, Coleman and Eling 2000, Carling *et al.* 2000, Maddux *et al.* 2003b, Gyr and Kinzelbach 2004, Schindler and Robert 2005, Best 2005). Nevertheless, the respective effects of grain movements, flow-bed instabilities and bed-wave-flow interactions on bed-wave generation and development processes continue to intrigue researchers and demand understanding to aid practical issues of fluvial engineering and management. Methods promoted to predict the types and sizes of bed waves occurring in equilibrium with a flow suffer significantly (ASCE 2002) from the lack of understanding of the physical mechanisms controlling bed-wave development to equilibrium. Numerical simulations of erodible-bed development similarly suffer (ASCE 2002) from a lack of appropriate turbulence models for bed waves developing to equilibrium. In particular, few studies have incorporated mobile-bed sediment-transporting flows. How the presence of truly mobile bed waves modifies the flow and *vice versa* is unknown and potentially may significantly change current understanding of these processes (e.g., Muste and Patel 1997, Best *et al*. 1997).

A three-year New-Zealand-government-funded project was begun in 2003 to advance understanding of subaqueous sand waves. The SWAT.nz (New-Zealand-based research into sand waves and turbulence) project combined two research teams, from The University of Auckland and from the National Institute of Water and Atmospheric Research (NIWA). The goal of the project was to clarify the most intriguing problem of submerged particulate waves: what causes these waves to form and grow.

This paper provides an overview of the SWAT.nz programme. With the noted paucity of detailed studies of sand-wave mechanics in mobile-bed sediment-transporting flows, the principal purpose of this paper is to provide insight with regard to programme, experiment and analysis design for such studies of mobile-bed turbulent-flow dynamics. Firstly, the programme philosophy and framework is outlined below. The design and details of the mobile-bed experiments of varying scales completed within the programme are then reviewed. The analysis philosophies and methodologies adopted for interpreting the complex measured data sets are also outlined and detailed. To illustrate the values of the SWAT.nz programme and the developed methodologies, example project findings to date are presented and discussed.

2. SWAT.nz RESEARCH PROGRAMME AND OVERALL METHODOLOGY

The main hypothesis of the SWAT.nz project is that sand-wave (dune and ripple) origin and development to equilibrium is controlled by multiple mechanisms arising from a complex combination of grain motion and flow hydrodynamics that evolves as a bed develops. As an example, this combination may change during bed-wave development from domination of local (at grain scale) effects at small development times to domination of non-local (e.g., hydrodynamic and turbulent) effects at large development times.

Wanting to address the noted absence of investigation of flow and bed development for sediment-transporting flows and naturally mobile and variable bed waves (e.g., Best 2005), the central focus of the programme was the measurement of the three-dimensional development of sand waves and the associated flow from plane-bed

conditions to equilibrium bed-form magnitudes in an extensive series of ninety-six experiments (Table 1). The erodible-bed experiments were carried out in two glass-sided tilting recirculating (water and sediment) laboratory flumes (measuring 0.44×0.38 (deep) ×12 m and 1.5×1.2 (deep) ×45 m, respectively) in the Fluid Mechanics Laboratory at The University of Auckland. Initially a small stream in the field was to be studied along with use of the smaller flume. The larger flume was selected in lieu of the stream as it provided the same scale of processes with markedly greater control over both flow and bed behaviour and also measurement procedures. The adopted combination of leading-edge measuring equipment and extensive data analyses utilising methods of deterministic and statistical fluid mechanics was planned to yield results providing insight into, and tests and validation of, the key mechanisms of particulate-wave generation and development.

Table 1

Experimental conditions. Each of the identified tests was undertaken in two stages (developing bed with flying probes, and equilibrium bed with stationary probes). Each stage was run twice for two sets of vertical ADV positions.

Flume width	H [m]	d [mm]	U [m/s]	u_* *(logvel)* [m/s]	u_* *(stress)* [m/s]	u_* *(slope)* [m/s]	S_e [%]	Test
Narrow 440(n)	shallow 0.15(s)	fine 0.24(f)	0.35	0.025	0.029	0.027	0.10	nsf10
			0.43	0.033	0.030	0.030	0.10	nsf125
			0.46	0.029	0.029	0.031	0.10	nsf14
			0.61	0.033	0.033	0.034	0.10	nsf18
		coarse 0.8(c)	0.57	0.046	0.044	0.033	0.17	nsc175
			0.62	0.050	0.048	0.038	0.23	nsc20
			0.67	0.050	0.050	0.045	0.27	nsc22
			0.72	0.048	0.057	0.051	0.30	nsc24
	deep 0.22(d)	fine 0.24(f)	0.38	0.038	0.029	0.022	0.10	ndf14
			0.47	0.044	0.030	0.024	0.10	ndf17
			0.56	0.061	0.030	0.026	0.10	ndf20
			0.65	0.045	0.037	0.029	0.10	ndf23
		coarse 0.8(c)	0.59	0.060	0.041	0.034	0.10	ndc225
			0.70	0.063	0.053	0.044	0.10	ndc275
			0.78	0.075	0.059	0.045	0.10	ndc305
			0.83	0.040	0.059	0.047	0.10	ndc325
Wide 1500(w)	shallow 0.15(s)	coarse 0.8(c)	0.37	0.051	0.033	0.060	0.29	wsc07
			0.41	0.051	0.037	0.056	0.35	wsc85
			0.46	0.068	0.034	0.061	0.39	wsc10
			0.54	0.089	0.044	0.070	0.43	wsc115
	deep 0.52(d)	coarse 0.8(c)	0.56	0.037	0.041	0.057	0.06	wdc25
			0.69	0.066	0.069	0.066	0.15	wdc30
			0.75	0.058	0.062	0.071	0.19	wdc33
			0.81	0.065	0.069	0.077	0.22	wdc35

Two series of fixed-bed studies were also carried out to provide initial tests of the sand-wave concepts and measurement methodologies developed within the programme. In the first series, flow over a fixed two-dimensional dune profile (a train of 15 sand waves) was measured for a range of flow depths of similar mean velocity. The dune profile measured 0.75 m long and 0.04 m in height (crest to trough), with a 30° lee slope and a cosine-shaped stoss slope, and with glued 0.8 mm sand covering the bedform surface. A second series of 11 experiments was undertaken to assess flow over two-dimensional transverse repeated square-rib roughness of varying spacing λ/h = 1-16 (roughness spacing/height ratio), with h/H = 0.09 (roughness height/flow depth). Details of the fixed-bed-experiment methodologies are given in Coleman *et al.* (2005a, 2006, and 2007) and will not be discussed further here.

3. MOBILE-BED EXPERIMENTAL DESIGN

3.1 Experimental series

The mobile-bed experiments undertaken are summarized in Table 1. The test codes shown indicate the flume width, (n)arrow or (w)ide, the relative flow depth, (s)hallow or (d)eep, the sand size, (f)ine or (c)oarse, and a numerical representation of the relative flow strength. For the wide-flume, mean flow depths H of 0.15 m and 0.52 m were tested for a uniform nonrippling sediment (Fig. 1b) of median size d = 0.8 mm. Mean flow depths of 0.15 m and 0.22 m were tested in the narrow flume for each of d = 0.24 mm (forming ripples, Fig. 1a, and dunes) and d = 0.8 mm, both uniform sediments. For each depth-sediment combination, a range of four subcritical flow strengths was tested. Scaling of sand waves with a variety of flow and sediment scales could be tested through the ranges of variables selected. In this regard, one set of the wide-flume tests was chosen to be of the flow depth of 0.15m adopted for the narrow flume, i.e. looking at possible channel-width effects. The second set of wide-flume tests was of a flow depth of 0.52 m giving the same aspect ratio as the 0.15 m deep flow in the narrow flume, i.e. looking at possible flow-depth effects. The values of depth-averaged velocity U given in Table 1 were obtained from integrating a logarithmic fit to measured flow data. Shear velocity u_* values were determined from all of a fit to the measured water-surface slope, a logarithmic velocity-profile fit, and the Reynolds stress at the sand-wave crests (defined by the roughness geometry function of Nikora *et al*. 2007a being equal to 0.95). S_e is the test equilibrium bed slope.

3.2 Experimental procedures

Prior to each test proper, the test was run over a long duration to give steady-state equilibrium-magnitude bed forms. In each case, the flume slope was adjusted with the bed development to determine the bed slope S_e giving uniform flow for the equilibrium sand-wave magnitudes. The bed was then flattened at this flume slope and the test proper, involving measurement of bed and flow development from initial plane-bed conditions, could begin.

Four-dimensional bed development was recorded for each test using a 31-transducer 5 MHz ultrasonic ranging system manufactured by Seatek. Flow profiles corresponding to the bed-morphology measurements were measured for each test using a suite of four Sontek 10 MHz 3D Acoustic Doppler Velocimeters (ADVs) connected to a single PC and operating synchronously (Fig. 2).

For each condition of Table 1, two procedures were used. For the bed developing from planar conditions to equilibrium sand-waves, "flying" probes measured continuously as they moved over the bed (e.g., Friedrich *et al.* 2005, Clunie *et al*. 2007). Stationary probes were used for propagating equilibrium sand waves. The flying-probe (moving-carriage) approach is ideal for the present application of measuring and interpreting a flow field that is varying in time and space. While the flow along the flume varies insignificantly in a bulk sense, irregular local variations due to the presence of moving, growing sand waves necessitate measurement of a large region in a short time. The flying-probe and stationary-probe procedures are discussed further in Sections 3.3 and 3.4.

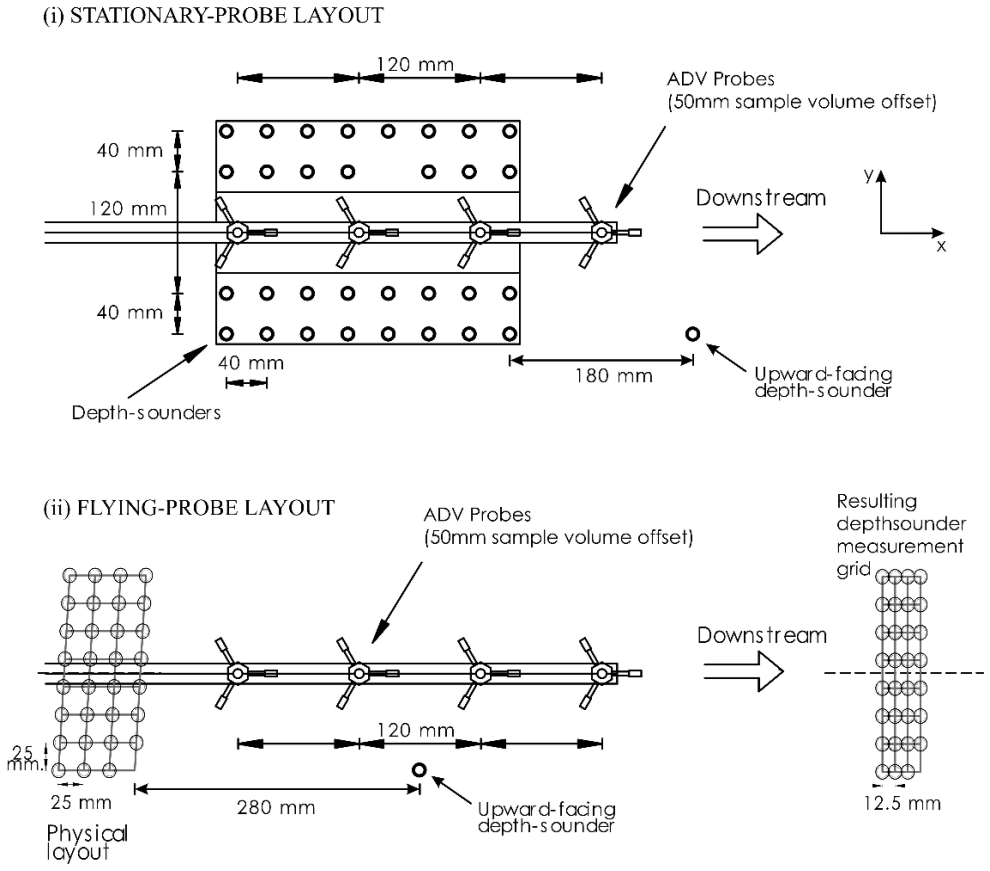

Fig. 2a. Sensor arrangements: narrow flume.

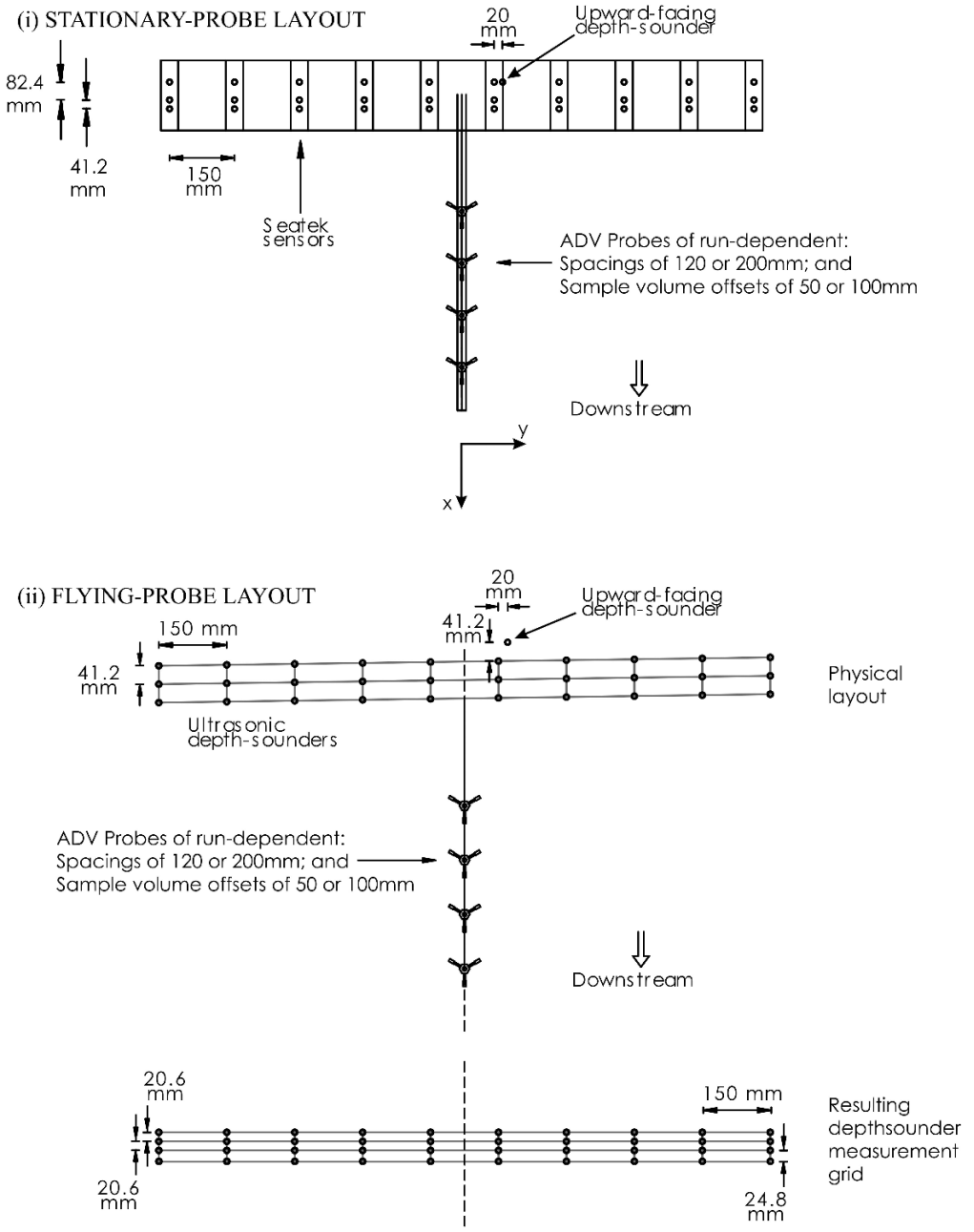

Fig. 2b. Sensor arrangements: wide flume. ADV spacings and sample-volume offsets (upstream to downstream probes): Series ‘wdc’ was of spacings of 200 mm, and offsets of 50, 50, 100 and 100 mm; Series ‘wsc’ (first ADV levels) was of spacings of 200, 120, and 120 mm, and offsets of 100, 50, 50, and 50 mm; and Series ‘wsc’ (second ADV levels) was of spacings of 120 mm, and offsets of 50 mm.

For the narrow-flume flying-probe tests, the chain-and-sprocket driven programmable-speed motorized carriage carrying the Seatek sensors and ADVs (Fig. 2a) moved at 250 mm/s for 25 s in each direction, with a 5 s dwell time between traverses. Analyses were only undertaken on data measured in the downstream direction of motion (i.e., every minute), with the Seatek array automatically lifted clear of the water for upstream motion (reducing any influence of the moving array on the erodible bed). The downstream carriage speed was less than the bulk flow velocity for each test. To synchronise the ADV and Seatek measurements, a fixed object that was sensed by both systems was placed on the flattened bed and traversed, and then removed prior to the pumps being started. Upstream and downstream microswitches (4.52 m apart) that were automatically triggered by the moving carriage were used to mark traverse durations (and carriage speeds) in the recorded data for subsequent analysis of the ADV records. Bed profiles were recorded and analysed over the full 6.25 m traversed. The passage of equilibrium sand waves and flow was subsequently continuously recorded using the stationary probes for periods of up to 14 hours.

Tests in the wide flume followed the procedures above. The rack-and-pinion-driven programmable-speed motorized carriage (of sensor arrangements as per Fig. 2b) moved upstream and downstream at 330 mm/s for 56 s (4 s dwell time), with analysis of the downstream results recorded every two minutes. The traverse-limit microswitches for the ADV analyses were spaced 14.614 m apart, with bed profiles analysed over the full 18.48 m traversed. The stationary-probe (Fig. 2b) measurements of equilibrium conditions were of durations of up to 6 hours.

3.3 Flow-field measurements

The four downward-looking ADVs used for the tests were aligned along the flume centreline and were positioned at set levels above and below the mean bed at the start of a test. The same centreline ADV levels and spacings were used for the developing and equilibrium phases of a test. Each experimental condition of Table 1 was repeated for two sets of ADV positions to give eight levels of flow information (within approximately two sand-wave heights of equilibrium trough levels) for each developing bed. ADV samples were recorded at 50 Hz, with seed particles required for ADV operation provided by naturally-occurring bed-sediment fines or artificially-seeded fine 8 μm hollow glass spheres. Standard ADV sample volumes were utilised (Clunie *et al.* 2007). These volumes were generally at offsets (Figs. 2a, b) of 50 mm from the probe, probes of 100 mm displacement distances being used to aid velocity measurement below the crests of large dunes. Horizontal probe spacings were 120 mm for the narrow flume (Fig. 2a), and 120-200 mm for the wide-flume tests (Fig. 2b). Probe alignments were checked before measurements were taken, with recorded velocities for a downstream still-water carriage flight checked to see that the measured average lateral velocity tended to zero. Probe vertical alignment was checked with a spirit level.

Using measurements of flows over fixed beds (flat and dune-shaped), the operation and limitations of the flying-ADV-probe system were confirmed by comparison

of flying-probe (measured as moving) results with equivalent results obtained using arrays of stationary-probe measurements at fixed positions (e.g., Clunie *et al*. 2007).

3.4 Bed-morphology measurements

Bed and free-surface elevations were measured by the 31-transducer 5 MHz Seatek system to within ±1 mm, with one of the transducers being used to map water-surface elevation (Figs. 2a, b), and the remainder being arranged to measure the three-dimensional morphology (Friedrich *et al.* 2005, 2006a). Individual transducers were polled at 5 Hz. Correct usage of the Seatek system, including operation and interpretation in flying mode, was verified using measurements over fixed bedforms (Friedrich *et al.* 2005).

For the narrow-flume flying-probe tests, the bed-sensing transducers were arranged in four rows (seven-eight probes along each row) across the flume (Fig. 2a), the carriage motion facilitating recording of eight continuous transects parallel to the flume centreline (Δx = 12.5 mm, Δy = 25 mm) for each probe sweep along the flume length. The wide-flume flying-probe bed-sensing transducers were arranged in three rows (ten probes along each row) across the flume (Fig. 2b), giving ten continuous transects parallel to the flume centreline, with Δx = 20.6-24.8 mm and Δy = 150 mm. For each flume, the probe positions along the flume were staggered so that regular measurement grids would be obtained when the carriage was moving and the Seatek probes were firing in sequence (Figs. 2a, b).

To aid probe correlation analyses for the stationary-probe tests, the narrow-flume bed-sensing probes were arranged in eight rows (three-four probes along each row) across the flume (Fig. 2a), with Δx = 40 mm, and Δy = 120 mm and 40 mm between the central and outer pairs of along-flume columns, respectively. For the wide-flume stationary-probe tests, the three probes within each of the ten along-flume columns were set at Δx = 41.2 mm and Δx = 82.4 mm (Fig. 2b), with Δy = 150 mm.

4. MOBILE-BED DATA-ANALYSIS STRATEGIES

The extensive data gathering resulted in a large database of flow and bed-geometry characteristics at various scales. In order to best utilise these data, a series of project-team workshops advanced theoretical and applied issues of data analysis and interpretation. As discussed below, data from the experiments were used to obtain quantitative measures of flow structure and bed morphology, and their interaction, as these developed.

4.1 Developing beds

For the flying-probe bed-development tests, carriage speeds were taken to be sufficiently large compared to bed-development rates that each recorded bed profile could be assumed to be representative of a static snapshot of the dynamically-changing bed. Each recorded flight of the ADVs was similarly taken to describe the flow at a particular stage of bed development (from flat bed conditions to the equilibrium-sized sand

waves). As will be seen, because the ADV-measured velocities during a flight varied in time and space, flight-averaged flow characteristics are double averages (in space and time), with deviations from these double-averaged quantities encompassing fluctuations in space and time.

4.2 Flow fields

Data processing

The measured ADV data were filtered to remove results of poor correlation or low signal-to-noise ratio (SNR). Phase-space despiking in terms of streamwise velocity (Goring and Nikora 2002) was similarly used to remove outlier (invalid) data points.

Comparisons of ADV records with measured bed topography were used to identify periods for which the ADV sample volume was in the bed, and for which recorded data were consequently to be removed. The bounds on these periods were precisely located by identification of associated boundary-induced spikes in measured SNR (Clunie *et al.* 2007).

Potential boundary-reflection interference of ADV measurements could not be avoided for the present measurements over greatly-varying bed levels. Data so affected were filtered out based on lowered ADV-measured correlation coefficients (Clunie *et al*. 2007). As a consequence, gaps in the filtered data record for an ADV probe could oftentimes be linked with the occurrence of problematic bed levels beneath the probe.

When required for analysis procedures (e.g., spectra and autocorrelation analyses, etc.), removed data points were replaced by linearly-interpolated values for gaps of up to 10 s, the data record being truncated for gaps of longer durations. Recorded streamwise flow velocity was corrected for the carriage motion. Properties of the measured flow fields were analysed based on the double-averaged (in time and in space) hydrodynamic equations (Nikora 2004, Nikora *et al.* 2007a, b) and statistical fluid mechanics.

Flow decomposition and the double-averaging methodology (DAM)

For flow over sand waves of characteristic sizes, scale-consistent flow and bed descriptions can be obtained by adopting a spatial-averaging framework for the flow field. In most practical cases of interest, the spatial averaging is carried out over a thin slab parallel to the mean bed with a planar extent typically chosen to be much larger than roughness or flow geometry scales (Fig. 3), but smaller than larger geometric features, such as channel curvature and widening or narrowing (Nikora *et al.* 2007a). Within this framework, instantaneous point velocities can be decomposed as

$$u_i = \overline{u}_i + u_i' = \langle \overline{u}_i \rangle + \tilde{u}_i + u_i' , \quad \langle \overline{u}_i \rangle = \frac{1}{V_f} \iiint_{V_f} \overline{u}_i \, \mathrm{d}V , \tag{1}$$

where u_i is the i-th component, in direction $x_i = (x, y, z)$, of the instantaneous velocity vector (u, v, w); the straight overbar and angled brackets represent time and spatial

averaging, respectively; $\langle \overline{u}_i \rangle$ is the double-averaged (in time and space) velocity; $\tilde{u}_i$ is the spatial fluctuation in the time-averaged velocity; $\langle \tilde{u}_i \rangle = 0$; u_i' is the temporal (turbulent) velocity fluctuation; and V_f is the volume occupied by fluid within a region R centred at level z with the total averaging volume V_0 (Fig. 3). Utilising this framework, the interaction between bed and flow can then be investigated at a primary level based on double-averaged flow properties.

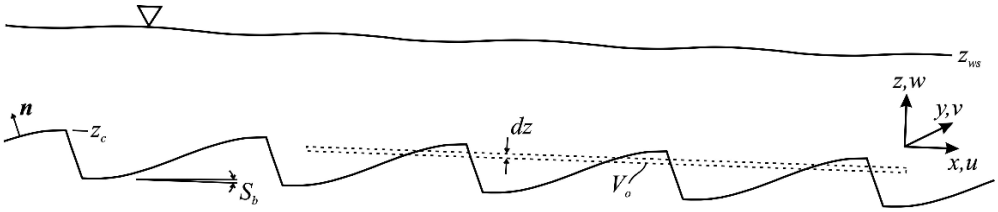

Fig. 3. Example averaging domain (shown as dashed lines) for a sand-wave bed.

To aid considerations of momentum transfer processes for sand waves, the Navier–Stokes equations can be averaged in time and space (Nikora *et al.* 2007a) to identify the key flow properties to be considered. For steady high-Reynolds number water flows over stationary (relative to the flow) bed waves (Fig. 3), the double-averaged momentum conservation equation for the longitudinal velocity $u_i = u$ can be presented in integral form (simply summing thin bed-parallel spatial-averaging slabs) as

$$g S_b \int_z^{z_{ws}} \phi \, \mathrm{d}z = \int_z^{z_{ws}} \left[\phi \left\langle \overline{u}_j \right\rangle \frac{\partial \langle \overline{u} \rangle}{\partial x_j} + \frac{1}{\rho} \frac{\partial \phi \langle \overline{p} \rangle}{\partial x} - \frac{\partial \phi \left\langle \tau_{1j} \right\rangle / \rho}{\partial x_j} \right] \mathrm{d}z - \int_z^{z_c} \frac{1}{V_o} \iint_{S_{\mathrm{int}}} \left[\frac{\overline{p}}{\rho} n_x - \nu \frac{\partial \overline{u}}{\partial x_j} n_j \right] \mathrm{d}S \, \mathrm{d}z \,, \tag{2}$$

where g is the gravitational acceleration; S_b is the mean bed slope; $\phi = V_f/V_0$ is the roughness geometry function ($1 \geq \phi \geq 0$); p is the point pressure; ρ is the fluid density; ν is the fluid kinematic viscosity; S_{int} is the surface area of roughness-fluid interface within the thin-slab averaging volume; n_i is the i-th component of the unit vector normal to the surface element dS and directed into the fluid; z_c is the uppermost (crest) level of the bed; z_{ws} is the water-surface level; the boundary resistance forces exist for $z \leq z_c$; the Einstein convention is adopted, which prescribes a summation over each repeated index; and the right-handed coordinate system is implied (Fig. 3), i.e., the x-axis (u velocity component) is oriented along the main flow parallel to the averaged bed, the y-axis (v velocity component) is oriented to the left bank, and the z-axis (w velocity component) is pointing towards the water surface.

Equation (2) can be seen to describe the flux of gravity-induced momentum (left-hand side of (2)) *via* spatially-averaged fluid stresses $\langle \tau_{1j} \rangle$, secondary currents and flow nonuniformity to the boundary, where the momentum is removed through form drag

and skin friction (last two terms of (2)) for the stationary boundary. The fluid stresses are $\langle \tau_{1j} \rangle = -\rho\left(\langle \overline{u'u'_j} \rangle + \langle \tilde{u}\tilde{u}_j \rangle\right)$, where viscous fluid stresses can be neglected; $-\rho\langle \overline{u'u'_j} \rangle$ are spatially-averaged Reynolds stresses; and $-\rho\langle \tilde{u}\tilde{u}_j \rangle$ are form-induced (dispersive) stresses that are analogous to Reynolds stresses but due to correlations of spatial variations rather than temporal fluctuations. The roughness geometry function ϕ, which varies from unity above the roughness crests ($z > z_c$) to a minimum within the channel bed, is a statistical measure of both the random geometry of the bed surface and the porosity, becoming analogous to the conventional porosity coefficient when evaluated below the lowest trough level.

As will be seen, the DAM framework is particularly valuable for describing and analyzing flows over sand-waves, including offering better definitions for flow uniformity, flow two-dimensionality, and bed shear stress (Nikora *et al.* 2007a).

Statistical fluid mechanics

It is important to note that for the flying-probe (sweeping time and space together) procedure, turbulent and form-induced fluctuations cannot be dissociated. For each of the eight measurement levels for each run, the flying-probe (developing-bed) ADV data were therefore analysed to give for each along-flume flight probability distributions of velocities $u_i = \langle \overline{u_i} \rangle + (\tilde{u}_i + u'_i)$ and their moments, i.e., double-averaged velocities $\langle \overline{u}_i \rangle$, and standard deviations, skewnesses and kurtoses in terms of combined $(\tilde{u}_i + u'_i)$ In addition, the sum of the double-averaged fluid stresses $\langle \tau_{1j} \rangle = -\rho\left(\langle \overline{u'u'_j} \rangle + \langle \tilde{u}\tilde{u}_j \rangle\right)$ was calculated, along with double-averaged structure functions (above bed-wave crests) for the velocity components.

For the equilibrium sand waves, data for each probe of a run (at varying levels above the mean bed) were discretised into two-minute windows, with each window being representative of a local section of a sand wave passing underneath while being long enough to ensure statistical robustness. For each window section, probability distributions of velocities $u_i = \overline{u}_i + u'_i$ and their moments were evaluated, i.e., time-averaged velocities $\overline{u}_i$, and standard deviations, skewnesses and kurtoses in terms of u'_i. In addition, Reynolds stresses $\left(\overline{u'_i u'_j}\right)$ were calculated, along with auto-correlation functions, second- and third-order structure functions, and auto-spectra for velocity components. Combining these space-dependent two-minute equilibrium-window results for a run gave for each stationary probe probability distributions of velocities $\overline{u}_i = \langle \overline{u}_i \rangle + \tilde{u}_i$ and their moments, i.e., double-averaged velocities $\langle \overline{u}_i \rangle$, and standard deviations, skewnesses and kurtoses in terms of $\tilde{u}_i$. In addition, separate double-averaged measures of Reynolds stresses $-\rho\langle \overline{u'_i u'_j} \rangle$ and form-induced stresses $-\rho\langle \tilde{u}_i \tilde{u}_j \rangle$ were calculated, along with auto-correlation functions, second- and third-order structure functions, and auto-spectra for velocity components.

4.3 Bed morphologies

Data processing

The flying-probe and stationary-probe bed profiles recorded for a test were filtered to improve data quality. At first, detected suspended particles and faulty signals were eliminated, then the bed-profile data were despiked, with unjustified jumps in the data removed based on jump magnitude and quantity of removed (and replaced) data. Acceptable variations in bed level between neighbouring points varied based on expected bedform height, ranging 10 to ~30 mm for the flying probes and 10 to ~60 mm for the stationary probes. The larger tolerance for the stationary probes was due to the slower sand-wave motion relative to the probes giving more significant noisy-data patches when these arose for these probes. Removed data points were replaced using linear interpolation. The second criterion was used to minimise durations of missing (and replaced) values in the data set such that the bed profile was acceptably represented by the final result. For each data set (of a flying-probe or stationary-probe arrangement for a test), threshold criteria values were adjusted to optimise the resulting data quality.

For the cleaned bed-development data, analyses were then based on the longitudinal profiles. Depending on the analysis approach, the ten (wide flume) or eight (narrow flume) longitudinal profiles of a traverse along the flume were analysed individually or as an ensemble average for the given development stage of the test. The stationary-probe profiles were similarly analysed individually or as ensemble averages. If flume-side-wall effects were determined to have influenced the outer longitudinal profiles, then these were omitted from the ensemble averaging.

Random-field approach

The project team considered a three-way approach to analysing bed-surface data, with bed waves represented as (1) deterministic features, (2) stochastic features, and (3) features with dual deterministic and stochastic properties. Within each approach, the surface nature can further be considered (a) continuous, (b) discrete or (c) dual continuous and discrete. Extensive tests of various techniques and methodologies showed that the random-field approach was most promising and this was therefore the main focus of the bed-morphology research.

For each run, flying-probe and stationary probe bed-profile data were analysed to give for each sweep over the bed (each bed snapshot) representative digital elevation maps (DEMS); probability distributions of bed elevations and their moments (means, standard deviations, skewnesses and kurtoses); 1D longitudinal spectra and coherence functions; 2D correlation functions; longitudinal and transverse structure functions (of varying orders); and 2D structure functions (of varying orders). Cross-correlation between snapshots was used to provide cross-correlation and 1D longitudinal coherence functions for the central profiles; 1D longitudinal time-shift spectra; and sand-wave celerities.

5. PROJECT RESULTS

As indicated above, the purposes of this paper are to overview the philosophy and details of the SWAT.nz programme, and thereby to provide insight into programme, experiment and analysis design for studies of mobile-bed flows and sand-wave morphologies. Methodological challenges addressed in the SWAT.nz programme are discussed in Sections 3 and 4. Example results are presented in this section to illustrate the values of the SWAT.nz programme and the developed methodologies. Results are presented in terms of mobile-bed processes, and flow-bed interaction and flow processes for fixed-bed roughness and erodible beds, respectively.

5.1 Mobile-bed processes

Ripples and dunes

Strong debates continue in the hydraulics and earth-sciences communities as to the natures and mechanics of, and differences between, ripples and dunes. The project experiments were designed to cover expected ripple and dune bed profiles, and also transitions between these bedforms as the beds developed for selected tests.

Skewness values for probability distributions of sand-wave bed elevations were found to provide valuable insight into classification of the respective natures of ripples and dunes and when transitions between these features occur (Friedrich *et al.* 2006b). Such a means of bed morphology classification can be of particular use in the field where assessment of the range of sediment and flow characteristics for alternative bedform classification schemes can prove difficult.

Sand-wave three-dimensionality

Central to sand-wave dynamics is the role of three-dimensionality (e.g., Best 2005), for example in increasing or decreasing flow resistance as sand waves grow and two-dimensionality becomes unsustainable. Maddux *et al.* (2003a, b) measured flows over fixed 3D bed forms arranged in regular patterns, finding flow resistance for the 3D dunes to be 50% larger on average compared to that for equivalent 2D dunes in similar flows. In contrast, Venditti (2003) found that irregular arrangements of dune crests reduce form drag. Consistent with both of these studies, Sirovich and Karlsson (1997) showed that irregular 3D patterns of protrusions reduce form drag, whereas regular 3D patterns enhance form drag. Whereas each of these studies involved fixed beds that could be precisely defined, the question arises as to how to mechanistically and objectively quantify the three-dimensionality of alluvial sand waves, e.g. in order to link bed topography with flow resistance, particularly for mobile beds of waves that vary markedly in space and time.

Based on the project analyses, the geometry (e.g. central ellipse orientation and axis dimensions, Fig. 4) of the 2D autocorrelation function when applied to sand-bed-elevation fields can provide an effective means of assessing the three-dimensionality of sand waves (Friedrich *et al.* 2006a). Potential effects on sand-wave form of channel side-walls and the channel aspect-ratio can thereby be quantitatively assessed through

application of this function to measured bed morphologies. More importantly, the results of these 2D autocorrelation analyses together with measures of flow resistance can potentially provide sought after insight into the role of mobile-bed sand-wave form on flow resistance.

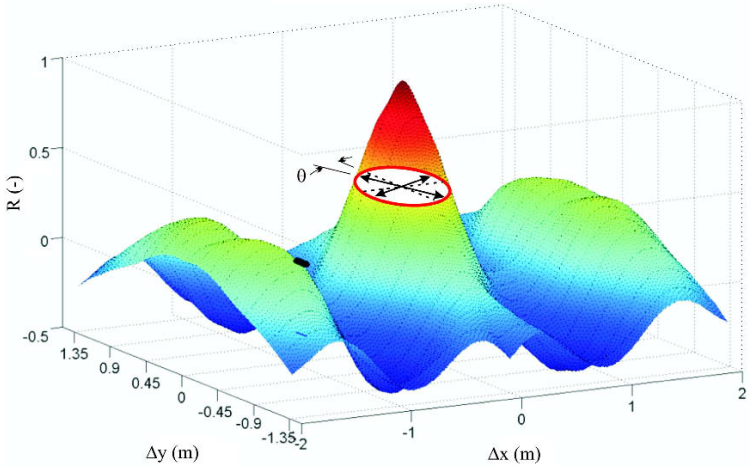

Fig. 4. Example 2D spatial autocorrelation function (minute 240 of Run wdc35) displayed for all four quadrants, with the central ellipse shown for a correlation level of 0.4. See colour version of this figure in electronic edition.

5.2 Fixed-bed flow-bed interaction and flow processes

Double-averaged velocities

For the square-rib fixed-bed tests (Coleman *et al.* 2005a, 2007), the double-averaged velocity profile was found to be (quasi) logarithmic above roughness tops, changing below roughness tops with increasing rib spacing from exponential ($\lambda/h < 10$) to linear ($\lambda/h \geq 10$) to logarithmic ($\lambda/h >> 10$), where λ/h is the roughness spacing/height ratio. Based on these results, a linear double-averaged velocity profile is expected below roughness tops for a typical sand-wave steepness of $\lambda/h \approx 20$. The project measurements.

over fixed dunes confirmed this expectation for developing bed waves and at equilibrium, with the interfacial-layer velocity profile predicted as (Fig. 5)

$$\langle \overline{u} \rangle / u_* = 11.0(z/h) + 4.1 \tag{3}$$

for a naturally-occurring dune steepness of $\lambda/h \approx 20$, where $z = 0$ is mean bed elevation and h is bed-wave height. Knowledge of this distribution below dune crests is notably useful for field investigations, for which measurements of sufficient resolutions below dune crests are typically difficult to obtain. Further research needs to be carried out, however, to complete generalization of this universal interfacial-layer profile for varying dune steepness. Project measurements also confirmed the existence of a conventional (quasi-) logarithmic velocity profile above sand-wave crests for developing bed waves and at equilibrium (Coleman *et al.* 2006).

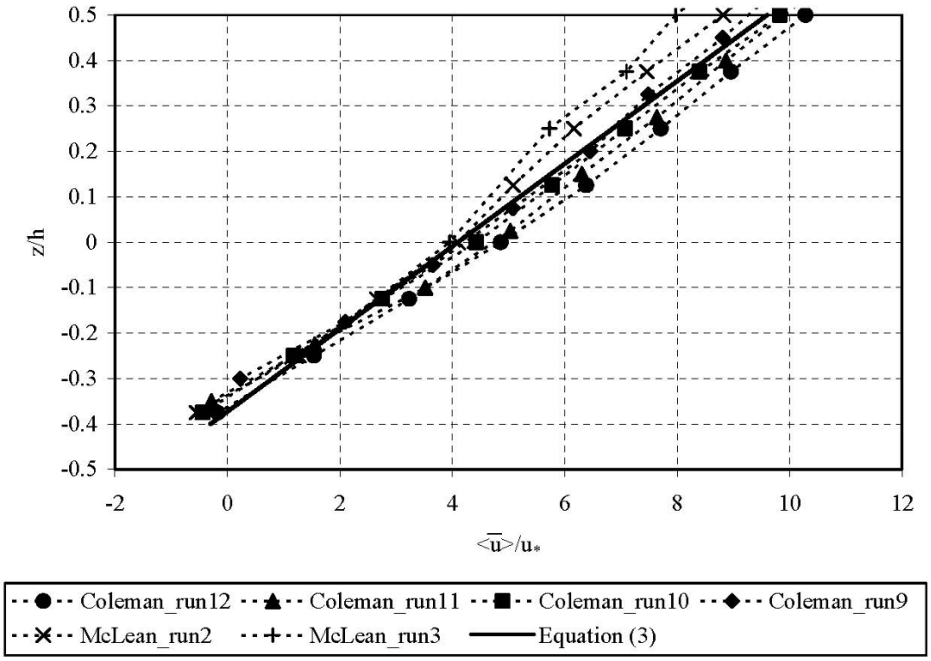

Fig. 5. Vertical distributions of double-averaged velocity within the interfacial layer for a dune steepness (height/length) of approximately 0.05. The data shown are from McLean *et al.* (1999) and Coleman *et al.* (2006), where the shear velocity values used for normalization have been obtained by extrapolation of the Reynolds stress profiles to the bed.

Momentum-flux components and balance

For steady uniform two-dimensional spatially-averaged flow with no secondary currents, as for the tested fixed dunes of Coleman *et al.* (2006), the momentum balance of (2) becomes:

$$\rho g S_b \int_z^{z_{ws}} \phi \, \mathrm{d}z = -\rho\phi \left\langle \overline{u'w'} \right\rangle (z) - \rho\phi \left\langle \tilde{u}\tilde{w} \right\rangle (z) - \int_z^{z_c} \frac{1}{V_0} \iint_{S_{\mathrm{int}}} \left[\bar{p} n_x - \rho\nu \frac{\partial \bar{u}}{\partial x_j} n_j \right] \mathrm{d}S \, \mathrm{d}z \,, \qquad (4)$$

where $\left\langle \overline{u'w'} \right\rangle (z_{ws}) = \left\langle \tilde{u}\tilde{w} \right\rangle (z_{ws}) = 0$, and Reynolds and form-induced stresses can be seen to transfer the gravity-induced momentum to the boundary where it is removed through form drag and skin friction.

Figure 6 presents the momentum flux components and balance of (4) for the Run 9 fixed 2D sand waves of Coleman *et al.* (2006), in which elevations are referenced to the mean bed elevation z_m, H is the mean flow depth, τ is the stress, and u_* is the shear velocity determined by extrapolation of the Reynolds stress profiles to the bed. The roughness geometry function $\phi(z)$ is also shown. The stress profile due to the gravity-induced momentum influx, "Gravity" in Fig. 6 (from the left-hand side of (4)), can be seen to vary linearly from zero at the water surface to the dune crests, and then

curve (defined by the ϕ roughness function) to a maximum, the bed shear stress, which occurs at the roughness trough.

In line with the indications of (4), at any level z, the total momentum efflux through flow and boundary effects ("Total" in Fig. 6) can be seen to balance the influx through gravity ("Gravity"), with decreasing flow effects and increasing boundary drag as z decreases from the roughness crests to the troughs. It is apparent that form-induced stresses can be significant, and that they act to balance variations in Reynolds stresses, particularly above roughness crests. These results and analyses highlight that knowledge of the effects of form-induced stresses, secondary currents, and flow non-uniformity can be particularly important for describing and modelling flows over sand waves.

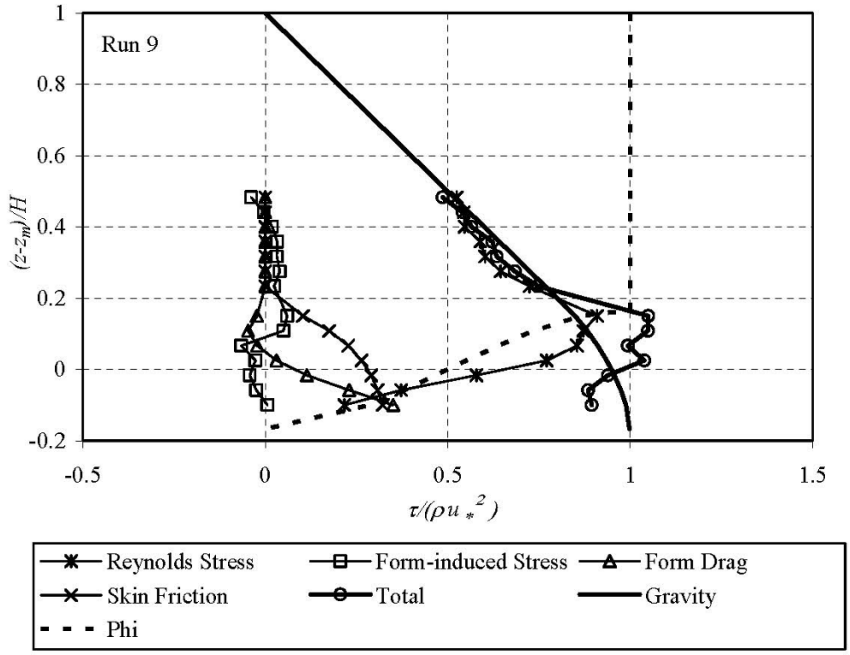

Fig. 6. Momentum flux components and balance for flow over fixed 2D sand waves (Run 9 of Coleman *et al*. 2006). Shown are the vertical distributions of Reynolds stress $-\rho\langle\overline{u'w'}\rangle\phi$, form-induced stress $-\rho\langle\tilde{u}\tilde{w}\rangle\phi$, form drag, skin friction, their sum (shown as "Total"), gravity-induced momentum, and the roughness geometry function ϕ.

Equilibrium nature of the sand-wave boundary layer

Recognising that dune steepness can be taken to be essentially invariant during the major period of growth (e.g. Niño *et al.* 2002, Coleman *et al.* 2005b), the measured flows of varying depth over the fixed sand waves of Coleman *et al.* (2006) provide insight into flow-dune interaction over the growth of a dune for the same flow. For the flows used of relatively low strengths and transport rates, and thereby low rates of erodible-boundary change in natural channels, a fixed-bed model can be justified for

flow simulation, with the natural bed essentially stationary with respect to the overhead low-strength flow.

The fixed-dune-bed project tests revealed a negligible variation in roughness layer (comprising the interfacial and form-induced layers, Nikora *et al*. 2007b) flow structure for developing dunes, i.e. an equilibrium boundary layer nature for flow over developing dunes. This result was confirmed in terms of spatial fields of time-averaged velocities and stresses, e.g. Fig. 7, where h is the sand-wave height, H is the mean flow depth, the spatial velocity fluctuation $\tilde{u}_i = \overline{u}_i - \langle \overline{u}_i \rangle$, $\langle \overline{u} \rangle$ below dune crests is given by Fig. 5, and u_* is the shear velocity determined by extrapolation of the Reynolds stress profiles to the bed. It was also evidenced by the Coleman *et al.* (2006) measured vertical distributions of: double-averaged (in time and space) longitudinal velocity (e.g. Fig. 5), double-averaged normal stresses, and the components of the momentum balance for the flow.

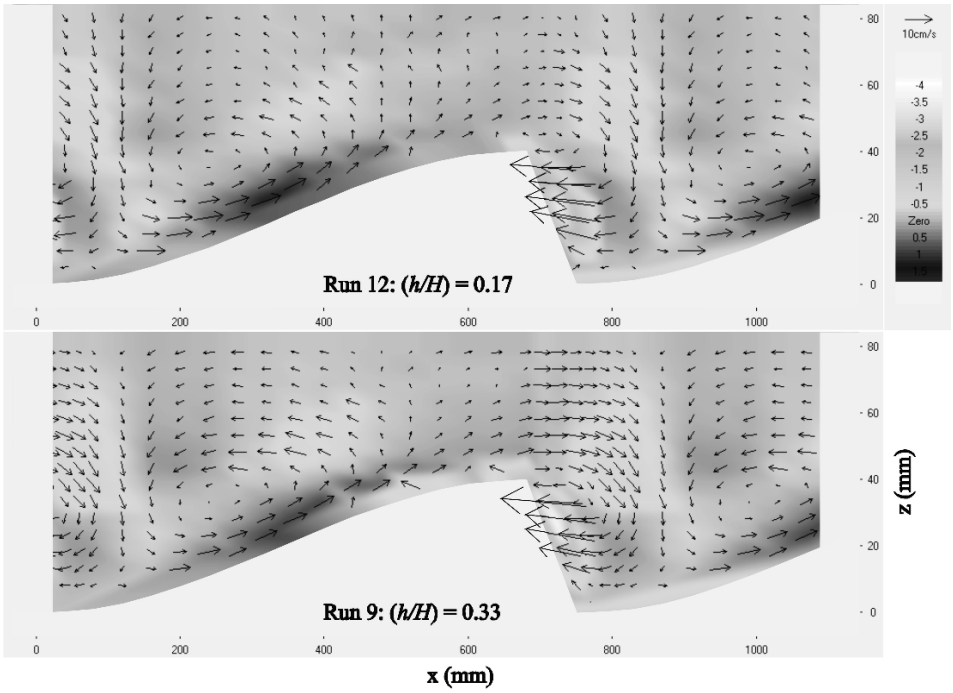

Fig. 7. Spatial fluctuations ($\tilde{u}$, $\tilde{w}$) in time-averaged velocities and contours of normalized (by ρu_*^2) form-induced stresses. Runs 9 and 12 of Coleman *et al.* (2006) represent equilibrium sand waves and developing waves at $t/t_e = 0.16$, respectively, where t_e is the time t required to achieve equilibrium conditions.

The finding of an equilibrium (self-similar) nature for the near-bed boundary layer over developing dunes with flow separation in the dune lee (Coleman *et al.* 2006) is significant in its centrality to understanding the feedback loop between flow, bed morphology and sediment transport that controls erodible-bed development.

5.3 Mobile-bed flow-bed interaction and flow processes

Bed and flow development results for the growing bed waves of mobile-bed test *ndf14* (Table 1) are shown in Fig. 8. The development of the bed configuration, from a flat bed to equilibrium-sized bedforms, is shown in Fig. 8a in terms of the standard deviation of bed elevations. Also presented are the associated developments for the run in both shear velocity and the double-averaged velocity at elevation $z = 0.046$ m above the mean bed level. Even this basic comparison of bed and flow development provides interesting insight, with the major hydrodynamic changes having occurred in the first ~50 minutes for the run, at which stage the slower-developing bedforms had reached perhaps 60% of their final height.

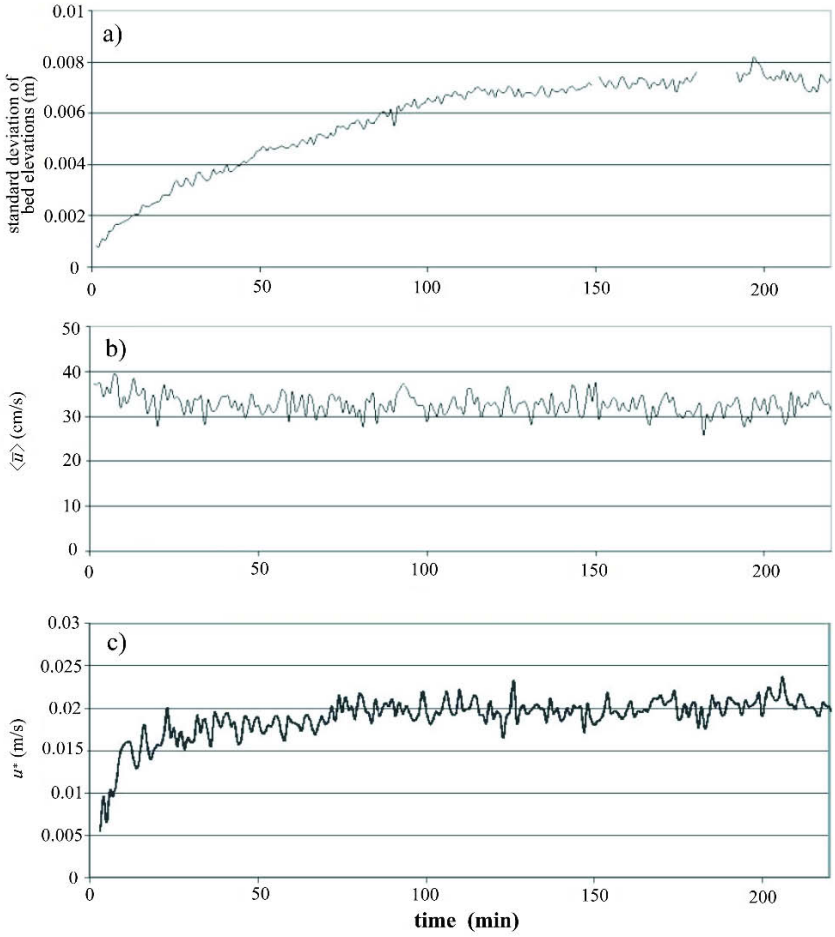

Fig. 8. Mobile-bed sand-wave development for Run ndf14 showing: (a) bed development in terms of standard deviation of bed elevations; (b) development of $\langle \overline{u} \rangle$ at an elevation of 0.046 m above the mean bed; and (c) development of shear velocity (determined from the measured water-surface slope).

Work continues on more detailed assessment of flow development with growing bedforms for the range of runs carried out, e.g., in terms of distributions of velocity moments and fluid stresses with depth, and along-flume correlations of turbulence characteristics with the bed profile. Work is also presently focusing on the effects on flow structure of sediment transport and three-dimensional flow and bed morphology. It is expected, however, that the boundary-layer flow structure patterns identified to date for the project fixed dunes will still be evident for the more complex natural systems.

6. CONCLUSIONS

The SWAT.nz research programme was carried out to advance understanding of subaqueous sand waves: principally, what causes these waves to form and grow. The research programme was based around detailed experimental studies, at stream and laboratory scales, with three-dimensional measurement of bed and associated flow development from plane-bed conditions to equilibrium sand-wave magnitudes recorded in a series of ninety-six experiments. Extensive data analyses were utilised to yield results providing insight into, and tests and validation of, the key mechanisms of particulate-wave generation and development.

The principal focus of this paper is to outline the philosophy and details of the SWAT.nz programme, and thereby to provide insight into programme, experiment and analysis design for studies of bed surfaces and flows that are highly variable in time and space, such as those occurring for sand waves. In this regard, as part of the programme design, "flying-probe" methodologies were developed to enable measurement and interpretation of bed surfaces and flows that are highly variable in time and space, e.g. flows over moving and growing three-dimensional bed waves. Flow measurements in time and space were made below sand-wave crests, aided by data processing methods devised to account for in-bed ADV measuring volumes and boundary-reflection interference for the varying levels of sand-wave surfaces. The data-analysis methodologies adopted for the measured beds and flows were centred on the double-averaged (in time and space) hydrodynamic framework and statistical analyses of the random fields of elevations and velocities.

The values of the SWAT.nz programme and the experiment and analysis methodologies developed and adopted are highlighted by the programme results to date. These results presented herein are in terms of mobile-bed processes, and flow-bed interaction and flow processes for fixed bed roughness and erodible beds, respectively. Work continues on using the measured project data to further reveal the effects of sediment transport and dynamically-changing natural sand waves on flow-bed interactions and flow processes.

Acknowledgements The SWAT.nz research programme was funded by the Marsden Fund (Grant No. UOA220) administered by the Royal Society of New Zealand. The writers wish to acknowledge the valuable contributions to the project of the technical staff, namely Glen Cooper, David Gunn, Jeremy Walsh and Katie Image of

NIWA, and Jim Bickner, Ray Hoffman, Geoff Kirby and Jim Luo of The University of Auckland. The writers also acknowledge Steve McLean's useful discussions and data provision, and the assistance with the fixed-bed studies of Ted Schlicke, Rebecca Lau, and Lowan Lou.

References

ASCE Task Force on Bed Forms in Alluvial Channels (1966), Nomenclature for bed forms in alluvial channels, *J. Hydraul. Div. ASCE* **92,** HY3, 51-64.

ASCE Task Committee on Flow and Transport over Dunes (2002), Flow and transport over dunes, *J. Hydr. Engrg. ASCE* **128**, 8, 726-728.

Bennett, S.J., and J.L. Best (1995), Mean flow and turbulence structure over fixed, two-dimensional dunes: implications for sediment transport and bedform stability, *Sedimentology* **42**, 491–513.

Best, J. (2005), The fluid dynamics of river dunes: a review and some future research directions, *J. Geophys. Res.* **110**, F04S02, DOI:10.1029/2004JF000218.

Best, J.L., S.J. Bennett, J.S. Bridge, and M.R. Leeder (1997), Turbulence modulation and particle velocities over flat sand beds at low transport rates, *J. Hydr. Engrg. ASCE* **123**, 1118-1129.

Carling, P.A., J.J. Williams, E. Gölz, and A.D. Kelsey (2000), The morphodynamics of fluvial sand dunes in the River Rhine near Mainz, Germany. Part II: Hydrodynamics and sediment transport, *Sedimentology* **47**, 253–278.

Clunie, T.M., V.I. Nikora, S.E. Coleman, H. Friedrich, and B.W. Melville (2007), Flow measurement using flying ADV probes, *J. Hydr. Engrg. ASCE* **133**, 12, 1345-1355.

Coleman, S.E., and B.W. Melville (1996), Initiation of bed forms on a flat sand bed, *J. Hydr. Engrg. ASCE* **122**, 6, 301-310.

Coleman, S.E., and B. Eling (2000), Sand wavelets in laminar open-channel flows, *J. Hydraul. Res. IAHR* **38**, 5, 331-338.

Coleman, S.E., V.I. Nikora, S.R. McLean, and E. Schlicke (2005a), Double-averaged turbulent flow over square-rib roughness, *4th IAHR Symposium on River, Coastal and Estuarine Morphodynamics*, *Urbana, IL, USA, 4-7 October 2005*, 211-216.

Coleman, S.E., M.H. Zhang, and T.M. Clunie (2005b), Sediment-wave development in subcritical water flow, *J. Hydr. Engrg. ASCE* **131**, 2, 106-111.

Coleman, S.E., V.I. Nikora, S.R. McLean, T.M. Clunie, E. Schlicke, and B.W. Melville (2006), Equilibrium hydrodynamics concept for developing dunes, *Physics of Fluids* **18***,* 10*,* 105104-1-12.

Coleman, S.E., V.I. Nikora, S.R. McLean, and E. Schlicke (2007), Spatially averaged turbulent flow over square ribs, *J. Engrg. Mech. ASCE* **133**, 2*,* 194-204.

Friedrich, H., B.W. Melville, S.E. Coleman, V.I. Nikora, and T.M. Clunie (2005), Three-dimensional measurement of laboratory submerged bed forms using moving probes, *XXXI IAHR Congress*, *Seoul, Korea, 11-16 September 2005*, 396-404.

Friedrich, H., B.W. Melville, S.E. Coleman, T.M. Clunie, V.I. Nikora, and D.G. Goring (2006a), Three-dimensional properties of laboratory sand waves obtained from two-dimensional autocorrelation analysis, *Int. Conf. on Fluvial Hydraulics*, *River Flow 2006*, *Lisbon, Portugal, 6-8 September 2006,* 1013-1022.

Friedrich, H., V.I. Nikora, B.W. Melville and S.E. Coleman (2006b), Statistical interpretation of geometric differences in ripple and dune shapes, *7th Int. Conf. on Hydroscience and Engineering*, *ICHE-2006*, *Philadelphia, USA, 10-13 September 2006*, 1-14.

Goring, D., and V. Nikora (2002), De-spiking ADV data, *J. Hydr. Engrg. ASCE* **128**, 1, 117-126.

Gyr, A., and W. Kinzelbach (2004), Bed forms in turbulent channel flow, *Appl. Mech. Rev.* **57**, 77-93.

Kostaschuk, R.A., and P.V. Villard (1996), Flow and sediment transport over large subaqueous dunes: Fraser River, Canada, *Sedimentology* **43**, 849-863.

Lyn, D.A. (1993), Turbulence measurements in open-channel flows over artificial bed forms, *J. Hydr. Engrg. ASCE* **119**, 3, 306-326.

Maddux, T.B., J.M. Nelson, and S.R. McLean (2003a), Turbulent flow over three-dimensional dunes: 1. Free surface and flow response, *J. Geophys. Res.* **108** F1, 6009, DOI:10.10 29/2003/JF000017.

Maddux, T.B., S.R. McLean, and J.M. Nelson (2003b), Turbulent flow over three-dimensional dunes: 2. fluid and bed stresses, *J. Geophys. Res.* **108** F1, 6010, DOI:10.1029/2003/ JF000018.

Marion, A., M. Bellinello, I. Guymer, and A.Packman (2002), Effect of bed form geometry on the penetration of non-reactive solutes into a stream bed, *Water Resour. Res* **38**, 10, 12 pp.

McLean, S.R., S.R. Wolfe, and J.M. Nelson (1999), Spatially averaged flow over a wavy boundary revisited, *J. Geophys. Res.* **104** C7, 15743-15753.

Muste, M., and V.C. Patel (1997), Velocity profiles for particles and liquid in open-channel flow with suspended sediment, *J. Hydr. Engrg. ASCE* **123**, 9, 742-751.

Nelson, J.M., S.R. McLean, and S.R. Wolfe (1993), Mean flow and turbulence fields over two-dimensional bedforms, *Water Resour. Res.* **29**, 3935-3953.

Nikora, V. (2004), Spatial averaging concept for rough-bed open-channel and overland flows. *Proc. Sixth Int. Conf. on Hydro-Science and Engineering*, *Brisbane, Australia*, 10 pp (CD).

Nikora, V.I. and D.M. Hicks (1997), Scaling relationships for sand wave development in unidirectional flow, *J. Hydr. Engrg. ASCE* **123**, 12, 1152-1156.

Nikora, V.I., A.N. Sukhodolov, and P.M. Rowiński (1997), Statistical sand wave dynamics in one-directional water flows, *J. Fluid Mech.* **351**, 17-39.

Nikora, V.I., I. McEwan, S.R. McLean, S.E. Coleman, D. Pokrajac, and R. Walters (2007a), Double-averaging concept for rough-bed open-channel and overland flows: theoretical background, *J. Hydr. Engrg. ASCE* **133**, 8, 873-883.

Nikora, V.I., S.R. McLean, S.E. Coleman, D. Pokrajac, I. McEwan, L. Campbell, J. Aberle, T.M. Clunie, and K. Koll (2007b), Double-averaging concept for rough-bed open-channel and overland flows: applications, *J. Hydr. Engrg. ASCE* **133**, 8, 884-895.

Niño, Y., A. Atala, M. Barahona, and D. Aracena (2002), Discrete particle model for analyzing bedform development, *J. Hydr. Engrg. ASCE* **128**, 4, 381-389.

Packman, A.I., M. Salehin, and M. Zaramella (2004), Hyporheic exchange with gravel beds: basic hydrodynamic interactions and bedform-induced advective flows, *J. Hydr. Engrg. ASCE* **130**, 7, 647-656.

Raudkivi, A.J. (1997), Ripples on a stream bed, *J. Hydr. Engrg. ASCE* **123**, 1, 58-64.

Schindler, R.J., and A. Robert (2005), Flow and turbulence structure across the ripple-dune transition: an experiment under mobile bed conditions, *Sedimentology* **52**, DOI: 10.1111/j.1365-3091.2005.00706x.

Sirovich, L., and S. Karlsson (1997), Turbulent drag reduction by passive mechanism, *Nature* **388**, 753-755.

Venditti, J.G. (2003), *Initiation and development of sand dunes in river channels*. Ph.D. Thesis, Department of Geography, University of British Columbia, 291 pp.

Yalin, M.S. (1992), *River Mechanics,* Pergamon Press Inc., New York.

Received 23 July 2007
Accepted 23 October 2007